Trajectory Tracking Control of a Nonholonomic Mobile Robot with Differential Drive

Rigoberto Luis Silva Sousa [#1], Marcus Davi do Nascimento Forte [#2],

Fabrício Gonzalez Nogueira [#3], Bismark Claure Torrico [#4]

[#] *Electrical Engineering Department, Universidade Federal do Ceará.*
Campus do Pici- s/n- Pici, Fortaleza, Brazil.
[1] `rigoberto@dee.ufc.br` [2] `davi2812@dee.ufc.br`
[3] `fnogueira@dee.ufc.br` [4] `bismark@dee.ufc.br`

Abstract— **This paper presents the development and trajectory tracking control of a nonholonomic mobile robot with differential drive. The used control system is composed of two loops cascaded, with internal PID controlling the speed of the two wheels and an external loop controlling the robot position and orientation. The second one is a feedfoward kinematics controller which is tuned according to desired closed-loop characteristics specified by the user. The control strategies were embedded in a digital module based in a 32-bit ARM microcontroller. In order to evaluate the performance of the developed robot, trajectory tracking tests were carried out for different trajectories and initial conditions. Preliminary experimental results are presented for reference trajectories without obstacles.**

Resumen — **Este artículo presenta la implementación práctica de un sistema de control para seguimiento de trayectorias de un robot móvil no holonómico de tracción diferencial. El sistema de control está basado en dos lazos, un lazo interno para el control de velocidad de las ruedas y un lazo externo para el control de la posición y orientación del robot. El lazo interno es controlado a través de dos controladores PID y dos encoders, por otro lado el lazo externo a través de un controlador cinemático prealimentado. El sistema de control es proyectado de acuerdo a especificaciones de lazo cerrado definidos por el usuario. La estrategia de control fue embarcada en microcontrolador ARM 32-bits con el fin de evaluar el desempeño del robot real. Fueron realizados varios experimentos de seguimiento de trayectorias con condiciones iniciales diferentes. Todos los experimentos fueron realizados considerando que no existen obstáculos.**

I. INTRODUCTION

The mobile robots belong to one of the most vast application areas in robotics, whether in exploration, observation, search and mapping many different enviroments [1].

From the perspective of control design, an important characteristic of mobile robots is the non-square dimensions of the models. This makes the task of designing their controller simpler because they commonly have only two variables (linear and angular speed) modelling the movement, but have three variables to model their position. The position variables are the (x,y) coordinates on a plane and the the angle the robot forms with the horizontal x axis

[1]. Therefore, there are fewer control variables than variables to be controlled.

The basic control of a robot in an environment can be made with a point-to-point approach (classic control), as the path of the states between the initial and final states are not important. The other possibility is to control the robot to make it follow a reference trajectory from its start point to the final point, which make it the most used approach, since the environments normally present obstacles [2].

The closed loop control is always used because it is robust to the initial states errors and other disturbances along the operation, which would not be possible in an open loop.

The path tracking control of mobile robots that have nonholonomic restrictions is an important problem in mobile robotics ([3], [4]). It consists mainly in assuring that the robot follows its predefined trajectory autonomously. In order to achieve the desired goal its necessary the use of sensors, actuators and embedded systems that allow the implementation of control technics dedicated to path tracking control [5].

The literature presents many proposals of nonholonomic wheeled mobile robots path tracking (WMR), the majority using the model based on the robot's kinematics equations, namely the kinematic model, because of its simplicity and because most robots have the linear and angular speeds as input parameters, and not acceleration or torque [2]. However other structures are also used. In [4] it is being used a linearization of the system's differential equations. In [6] the model is linearized considering the error between the reference robot and the real robot.

Nonholonomic systems normally have feedfoward control in which the system's input are calculated from the known trajectory and all the kinematics restrictions are implicitly treated in the trajectory's path ([2], [7], [8]).

This paper presents the preliminary results for the development of a real robot with a differential drive. To evaluate the robot's performance, a kinematic controller with feedforward action was used.

This paper is organized in the following way: in section II a physical description of the mobile robot is made, in section III the mathematical modeling is presented, in section IV the control strategy is presented, in sections V

and VI simulation and experimental results are presented, and the last section is a brief conclusion.

II. DESCRIPTION OF THE MOBILE ROBOT

The real mobile robot developed in this work is presented in Fig. 1. It is a wheeled differential drive mobile robot employed to evaluate the proposed control method. It has a height of 0.48m and a radius of 0.29m.

A bottom view of the of the robot's base is shown in Fig. 1.b The two larger wheels are driven by geared DC motors and the two smaller wheels are responsible for the equilibrium of the robot. The angular position of the wheels is measured through incremental encoders coupled to the motor shaft. The distance L between the two driven wheels is 0.4 m and the radius of the wheels is 0.08 m.
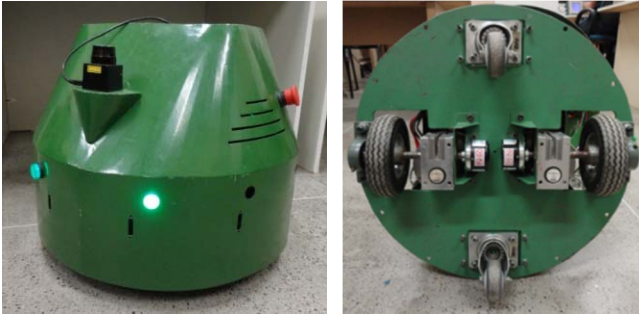

Fig. 1 a) Front View of Robot. b) Bottom view of the base assembly robot.

Fig. 2 shows a block diagram of the control circuits. The speed of the DC motors are controlled through PID controllers already included in the electronic driver. The PIDs were tuned with the following gains: proportional = 5.0, integral = 10.0 and derivative = 0.0. These values were set in order to achieve an over-damped closed loop response with rise time of 0.1 seconds. The speed feedback is obtained through incremental encoders coupled to the shaft.

The path tracking control strategy was implemented in an FRDM-K64F, a 32 bits ARM based board. The robot circuits and components are powered by a battery bank of 24V/45A and a 24/5V DC/DC converter. A second FRDM-K64F is connected to a supervisory computer which sends and receives data in real time though a wireless communication.
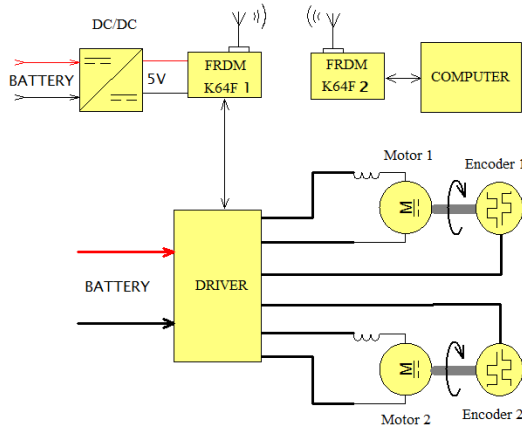

Fig. 2 Diagram Control circuit blocks.

III. MODELING OF MOBILE ROBOT

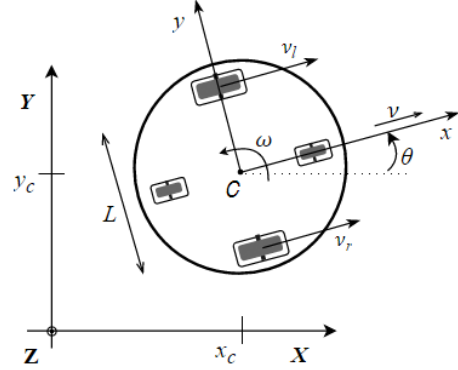The architecture of the robot together with their symbols are shown in Fig. 3.

Fig. 3 Architecture and symbols Robot.

It is supposed that its geometric center and the gravity center are coincident, and L is the distance between the two driven wheels. It is important to notice that C is the origin (x, y) and the center position between the two wheels, and θ is the orientation of the robot with respect to the axis (X, Y). Using the position coordinates and the orientation, it is possible to find the absolute (X,Y) coordinates in the absolute reference.

The velocity of the left (v_l) and right (v_r) wheels can be described respectively by:

$$v_l = v - \frac{\omega L}{2} \tag{1}$$

$$v_r = v + \frac{\omega L}{2}. \tag{2}$$

From Eqs. (1) and (2), the linear and angular velocities (v and ω respectively) can be obtained by:

$$v = \frac{v_l + v_r}{2}. \tag{3}$$

$$\omega = \frac{(v_r - v_l)}{L}. \tag{4}$$

Robots with this architecture have a constraint resulting from the machine's inability to move in the lateral direction of the wheel. This constraint is expressed in Eq. (5)

$$[- \sin \theta(t) \ \cos \theta(t)] \begin{bmatrix} \dot{x} \\ \dot{y} \end{bmatrix} = 0 \tag{5}$$

Consequently, the robot cannot move in the lateral direction of the wheel, and then the kinematic model is given by:

$$\begin{bmatrix} \dot{x}_c \\ \dot{y}_c \\ \dot{\theta}_c \end{bmatrix} = \begin{bmatrix} \cos \theta & 0 \\ \sin \theta & 0 \\ 0 & 1 \end{bmatrix} \cdot \begin{bmatrix} v \\ \omega \end{bmatrix} \tag{6}$$

For a given reference trajectory represented by $p_r(t) = (x_r(t), y_r(t), \theta_r(t))^t$, defined in a time interval $T \in [0, T]$, and from the inverse kinematics of the robot, a feedforward control law can be derived. However, these calculated inputs just can drive the robot in a desired path if there are no disturbances (slipping and skidding) and errors in the initial state.

The necessary robot inputs, tangential (v_r) and angular (ω_r) velocities, are calculated from the reference trajectory.

Therefore the reference tangential velocity is:

$$v_r(t) = \pm \sqrt{\dot{x}_r^2(t) + \dot{y}_r^2(t)}, \qquad (7)$$

where the signal $\pm$ is dependent on the desired direction of traction (+ forward and - backward) and the angular velocity of the robot is calculated from:

$$\omega_r(t) = \frac{\dot{x}_r(t)\,\ddot{y}_r(t) - \dot{y}_r(t)\ddot{x}_r(t)}{\dot{x}_r^2(t) + \dot{y}_r^2(t)}. \qquad (8)$$

The angle of each tangent point on the path is defined as:

$$\theta_r(t) = arctan2(\dot{y}_r(t), \dot{x}_r(t)) + k\pi, \qquad (9)$$

where k defines the desired direction (0 for forward and 1 for reverse) and arctan2 function is the inverse tangent function that returns the correct angles in all situations.

IV. CONTROLLER DESIGN

The concept of trajectory tracking error using two postures (robot position and orientation) can be seen in [4], where a reference posture is compared with the posture of the real robot. In [2] the reference robot is an imaginary robot which ideally follows the reference trajectory and the real robot has some errors with respect to the imaginary robot, as shown in Fig. 4.

The reference robot posture can be represented by $q_r = (x_r, y_r, \theta_r)^t$, and the posture of the real robot by $q = (x, y, \theta)^t$. The error between the two patterns is represented by $q_e = (e_1, e_2, e_3)^t$ and is written as:

$$\boldsymbol{q_e} = (\boldsymbol{q_r} - \boldsymbol{q}) \;\; or \;\; \begin{bmatrix} e_1 \\ e_2 \\ e_3 \end{bmatrix} = \begin{bmatrix} x_r - x \\ y_r - y \\ \theta_r - \theta \end{bmatrix}. \qquad (10)$$

Therefore, the control algorithm must be designed to force the real robot to accurately follow the reference trajectory.

Considering the rotation matrices of the two postures with respect to the Cartesian axis X and Y, the error can be represented as in Equation (11):

$$\begin{bmatrix} e_1 \\ e_2 \\ e_3 \end{bmatrix} = \begin{bmatrix} \cos\theta & \sin\theta & 0 \\ -\sin\theta & \cos\theta & 0 \\ 0 & 0 & 1 \end{bmatrix} . \begin{bmatrix} x_r - x \\ y_r - y \\ \theta_r - \theta \end{bmatrix}. \qquad (11)$$

Considering Eq.(11) and the kinematics of the robot in Eq. (6) the following kinematic model is obtained
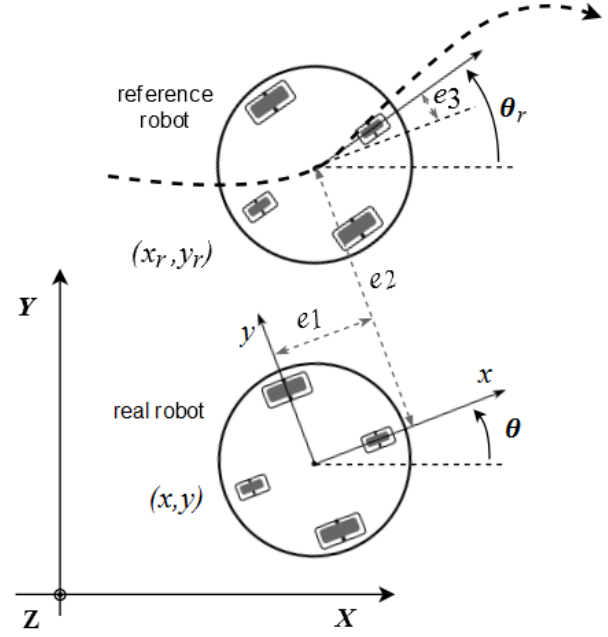

Fig. 4. Robot transformation error.

$$\begin{bmatrix} \dot{e}_1 \\ \dot{e}_2 \\ \dot{e}_3 \end{bmatrix} = \begin{bmatrix} \cos e_3 & 0 \\ \sin e_3 & 0 \\ 0 & 1 \end{bmatrix} . \begin{bmatrix} u_{r1} \\ u_{r2} \end{bmatrix} + \begin{bmatrix} -1 & e_2 \\ 0 & -e_1 \\ 0 & -1 \end{bmatrix} . \begin{bmatrix} u_1 \\ u_2 \end{bmatrix} \qquad (12)$$

where $u_{r1} = v_r$ and $u_{r2} = \omega_r$ are feedforward tangential and angular velocities, respectively. The robot inputs are defined as ([2], [4]):

$$\begin{aligned} u_1 &= u_{r1}\cos e_3 - v_1 \\ u_2 &= u_{r2} - v_2 \end{aligned} \qquad (13)$$

where $u_{r1}\cos e_3$ is the feedforward input, while v_1 and v_2 are the inputs of the closed loop circuit. From Eq. (13) expressing the closed loop input and rewriting Eq. (12) results in

$$\begin{bmatrix} \dot{e}_1 \\ \dot{e}_2 \\ \dot{e}_3 \end{bmatrix} = \begin{bmatrix} 0 & u_2 & 0 \\ -u_2 & 0 & 0 \\ 0 & 0 & 0 \end{bmatrix} . \begin{bmatrix} e_1 \\ e_2 \\ e_3 \end{bmatrix} + \begin{bmatrix} 0 \\ \sin e_2 \\ 0 \end{bmatrix} . u_{r1} + \begin{bmatrix} 1 & 0 \\ 0 & 0 \\ 0 & 1 \end{bmatrix} . \begin{bmatrix} v_1 \\ v_2 \end{bmatrix} \qquad (14)$$

Further linearizing Eq. (14) around the operating point OP (OP: $e_1 = e_2 = e_3 = 0$, $v_1 = v_2 = 0$) results in the following linear model:

$$\Delta\,\dot{e} = \begin{bmatrix} 0 & u_{r2} & 0 \\ -u_{r2} & 0 & u_{r1} \\ 0 & 0 & 0 \end{bmatrix} . \Delta_e + \begin{bmatrix} 1 & 0 \\ 0 & 0 \\ 0 & 1 \end{bmatrix} . \Delta\,v \qquad (15)$$

Eq. (16) can be written as: $\Delta\,\dot{q} = \mathbf{A}.\Delta\,\dot{q} + \mathbf{B}.\Delta\,\mathbf{u}$. The controllability matrix has full rank (B, AB, A²B) = 3 if any u_{r1} or u_{r2} is different from zero which is a sufficient condition for controllability only when the reference inputs u_{r1} and u_{r2} are constant.

The system defined by Eq.(6) is completely nonholonomic, it has only one nonholonomic constraint $\dot{y}_c\cos\theta - \dot{x}_c\sin\theta = 0$(the robot cannot move in the lateral direction of the wheel) and therefor the system is controllable.

We will later set the driver in a linear state space closed circuit. The system has three states and two inputs, so the gain matrix K has dimensions 2×3. The defined control scheme is illustrated in Fig. 5.
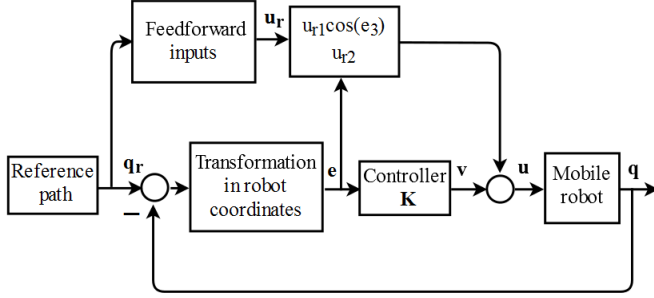

Fig. 5 Mobile robot control schematic.

$$v = K.e \qquad (16)$$

The controller structure can be derived from the observation of Fig. 4. To reduce the error in the direction of e_1 the tangential velocity of the robot must be changed accordingly. Likewise, the orientation error e_3 can be efficiently handled by the angular velocity of the robot. Finally, the error orthogonal to the driving direction can be reduced by changing the angular speed. At the same time, also the robot drive direction (forward or backward) must be considered. The adopted control law is:

$$\begin{bmatrix} v_1 \\ v_2 \end{bmatrix} = \begin{bmatrix} -k_1 & 0 & 0 \\ 0 & -sign\,(u_{r1})k_2 & -k_3 \end{bmatrix} \cdot \begin{bmatrix} e_1 \\ e_2 \\ e_3 \end{bmatrix} \qquad (17)$$

According to [2] and [4], the tuning of the controller gains is performed as a pole placement approach, comparing the real characteristic polynomial with a desired one. The desired polynomial is based on a second order system with desired relative damping and natural frequency:

$$(\,s + 2\zeta\omega_n\,)(\,s^2 + 2\zeta\omega_n s + \omega_n^2\,). \qquad (18)$$

An auxiliary pole at s = -2$\zeta\omega_n$ increases the rise time and decreases the overshot.

The characteristic closed loop polynomial is given by:

$$\det(\,s\,\mathbf{I} - \mathbf{A} + \mathbf{BK}) = s^3 + (\,k_1 + k_3)s^2 + \\ + (\,k_1 k_3 + k_2\,u_{r1} + u_{r2}^2)s + k_1 k_2\,eu_{r1} + k_3 u_{r2}^2 \qquad (19)$$

Using Eqs. (18) and (19) the solution can be obtained through:

$$k_1 + k_3 = 4\,\zeta\omega_n \\ k_1 k_3 + k_2\,u_{r1} + u_{r2}^2 = 4\zeta^2\omega_n^2 + \omega_n^2 \qquad (20)$$

$$k_1 k_2\,u_{r1} + k_3\,u_{r2}^2 = 2\zeta\,\omega_n^3$$

According to [2] and [4] the controller gains are given by:

$$k_1 = k_3 = 2\zeta\omega_n(t) \\ k_2 = g.|u_{r1}(t)| \qquad (21)$$

where:

$$\omega_n(t) = \sqrt{u_{r2}^2 + gu_{r1}^2(t)} \qquad (22)$$

The parameter g > 0 gives an additional degree of freedom to the controller project. It is important to notice that ω_n must be greater than the maximum allowed angular velocity of the robot, so $\omega_n \geq \max(u_{r2})$. A stability analysis and proof are presented in [2].

V.   SIMULATION RESULTS

This section shows simulation results of the path-tracking control strategy. The parameters of the non-linear kinematic controller are presented in Table 1. It is important to notice that these values were chosen after some tests with different sets of parameters. The resultant responses were evaluated and the better one was selected.

TABLE 1

VALUES OF THE CONTROLLER PARAMETERS

Variable	Value	Variable	Value
ζ	0.2	k1	0.8
ω_n	2.0	k2	3.0
g	30.0	k3	0.8

The used reference trajectory has a square form, as illustrated in Fig. 6. In order to enforce an initial posture error, the initial posture of the robot was set as $p_r(0) = [\,0.0, -0.5, 0.0]$.
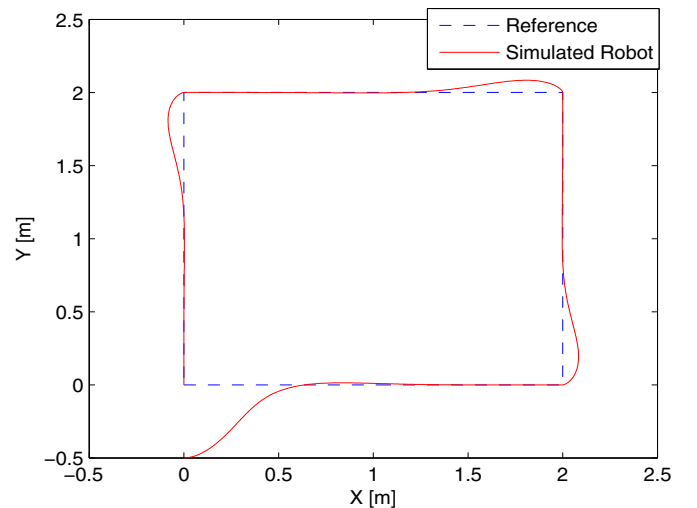

Fig. 6 Closed-loop control of simulated robot.

The reference path was generated setting v_r constant in 0.1m/s and ω_r initial equal to zero. In order to build the corners of the reference square, were made instantaneous variations of 90 degrees in θ at 20 s ($\theta = \pi/2$ rad), 40 s ($\theta = \pi$ rad) and 60 s ($\theta = 3\pi/2$ rad).The total time of the simulation was 80 s and the sampling time was set as 0.1 s.

The behavior of the linear and angular velocities of the robot are presented in Fig. 7 and the errors of postures during following-up the trajectory is presented in Fig. 8.
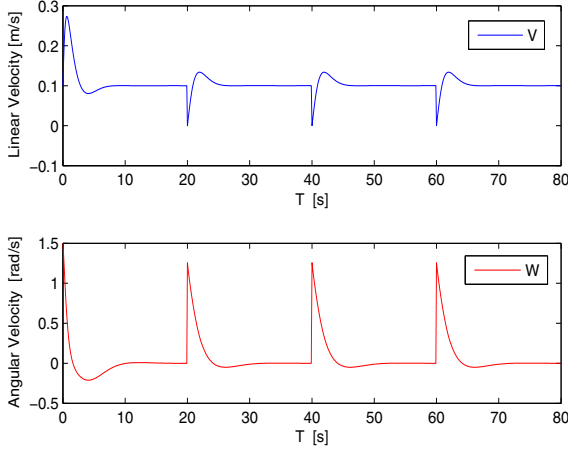
Fig. 7 Linear and angular velocities.
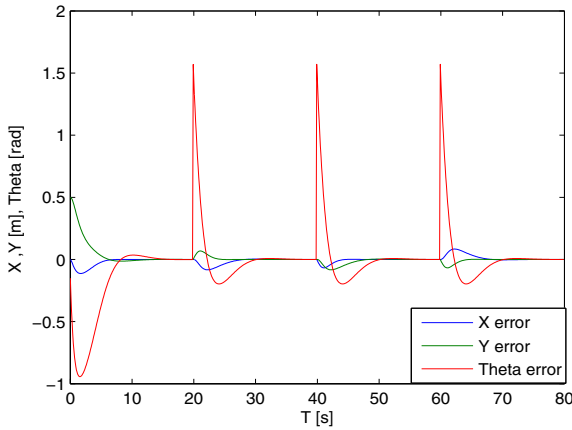
Fig. 8. Error variable in closed loop.

VI.   EXPERIMENTAL TESTS IN THE REAL ROBOT

The experimental tests were made in the mobile robot presented in Fig. 1. Two reference paths were used, the first is the same trajectory of the simulations, as shown in Fig. 9. The values of the controller parameters were the same used in the simulation tests.

In Fig. 9 is presented the trajectory tracking response in the XY plane. Note that the robot follows the reference path with a small position overshoot in the corners of the square. The behavior is very close to the obtained simulation results. Therefore, it shows that the developed models have good representation of the real mobile robot.

The linear and angular velocities of the robot obtained by the odometry algorithm with the output data of the encoders are presented in Fig. 10. As the previously figure, the

responses are close to the simulation results, but a natural noise can be seen. It can also be noticed that the robot speed did not saturate along the proposed trajectory.

Through Fig. 11 is possible to seen that the posture errors converge to zero after the transitory variations. It is important to notice that with other values for ζ, ω_n, and g an improved response can be obtained. Some tests showed that the closed-loop response is sensitive with the reference trajectory.
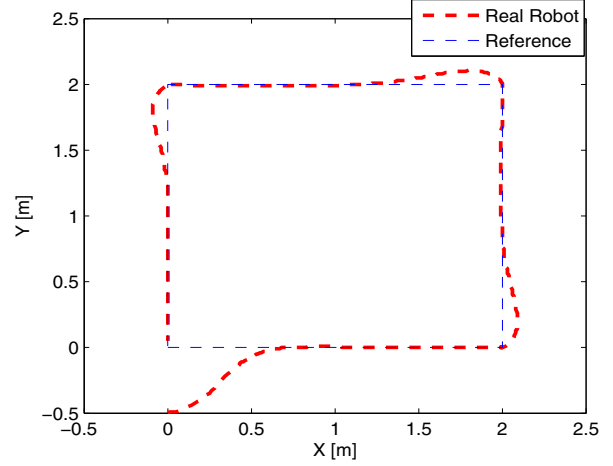

Fig. 9 closed-loop trajectory tracking test.
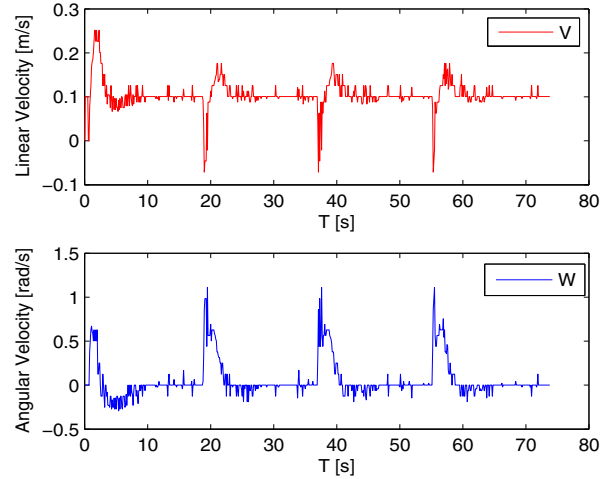

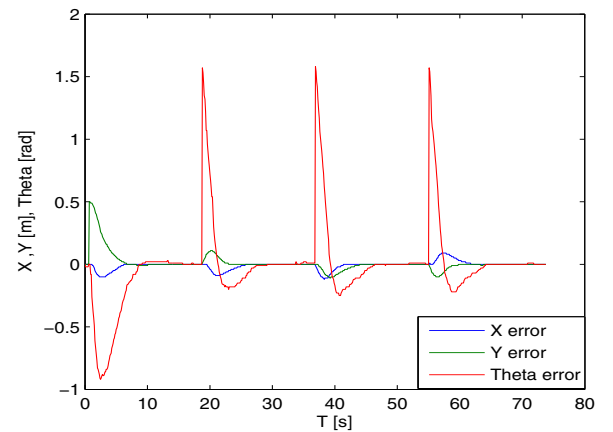Fig. 10 Linear and angular velocities of the real robot.

Fig. 11. Error robot trajectory tracking closed-loop.

The second reference path was generated using v_r constant equal 0.2 m/s and setting $\omega_r = 0.0$ at 15 s (0.025 rad/s), $\omega_r = 15.0$ at 27 s (0.30 rad/s), $\omega_r = 27.0$ at 36 s (-0.14 rad/s), and $\omega_r = 36.0$ at 47,2 s (0.287 rad/s). The total time of the test was 47.2 s and the sampling time was set as 0.1 s.

In this case, the initial position of the reference was adopted $p_r(0) = [\ 0.0,\ 0.0,\ -0.2]$ and the robot $p(0) = [\ 0.0, -0.5, 0.0]$. It is observed in Fig. 12 that after a small overshoot the robot followed the path satisfactorily.
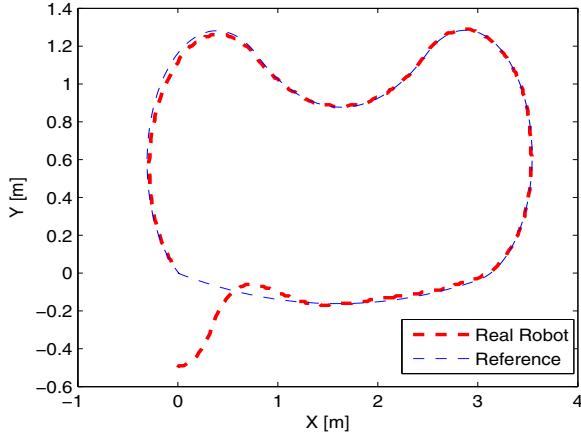

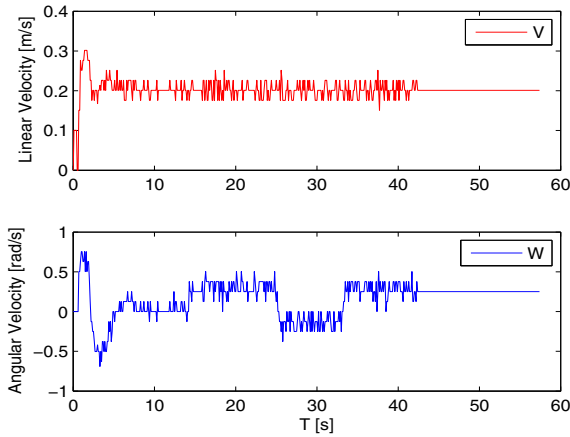Fig. 12 closed-loop trajectory tracking test.

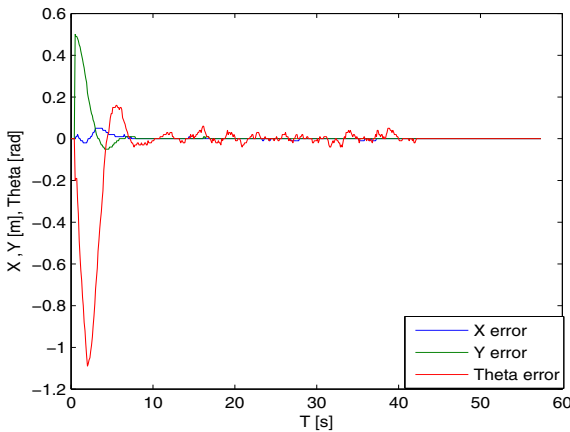Fig. 13 Linear and angular velocities of the real robot.

Fig. 14 Trajectory tracking error of the closed-loop test.

The linear and angular velocities of the robot (robot outputs) measured through the encoders are shown in Fig. 13. After the initial transient caused by the difference of posture, the signals tend to achieve the reference.

Through Fig. 14 is possible to see that the posture errors converge to zero after the transitory variations. Small oscillations around zero occurs due to noise and disturbances in the real control loops of the mobile robot.

VII.   CONCLUSIONS

The simulation and experimental tests presented in this work shown that the developed robot obtained satisfactory results to the tracking trajectory problem considering the two analyzed paths. The experimental results were very close to the simulation results, which is an indicative of good performance of the models. The authors believe that the mobile robot is able to more advanced control strategies, such as predictive and adaptive control.

During all tests were not observed slipping and skidding effects on the wheels. Strategies to deal with these effects are desirable, but were not assessed in this work.

VIII.   ACKNOWLEDGMENTS

REFERENCES

[1] Q. Zheng and Z. Gao, "Motion Control Design: Problem and Solutions," *Internation Journal of Intelligent Control and Systems, Vol. 10 no. 4,* pp. pp. 269-279, 2005.

[2] G. klancar, D. Matko e S. Blazic, "Mobile Robot Control on a reference Path," *Proceedings of the 2005 IEEE International Symposium on, Mediterranean Conference on Control and Automation ISSN 2155-9860,* pp. 1343-1348, 2005.

[3] L. Kalmanovsky and N. H. McClamroch,, ""Developments in Nonholonomic Control Problems,"," *IEEE Control Systens,* vol. 15, no. no. 6, pp. pp. 20-36, 1995.

[4] Y. Kanayama , Y. Kimura, F. Miyazaki e T. Noguchi, "A Stable Tracking Control Method for an Autonomous Mobile Robot," *Dudlex Knox Library,* pp. 384 - 389, 1990.

[5] A. A. D. d. Medeiros... [et al.], Robótica Móvel, São Paulo: LTC, 2015.

[6] F. Kuhne, W. . F. Lages and J. d. S. M. G. d. Jr, "Model Predictive Control of a Mobile Robot Using Linearization," in *In: 4th Mecatronics and Robótics*, Aachen, 2004.

[7] C. Canudas e Q. J. Sordalen, "Exponential Stabilization of Mobile Robots with Nonholonomic Constraints," *IEEE Transactions on Automatic Control,,* vol. 37, n. 11, pp. 1791-1797, 1992.

[8] S. Nicosia, B. Siciliano, A. Bicchi e P. Valigi, Articulated and Mobile Robotics for Services and Technologies, Berlin: Springer-Verlag, 2001.

[9] S. Blazic e M. Bernal, "Trajectory Tracking for Nonholonomic Mobile," em *Preprints of the 18th IFAC World Congress*, Milano, 2011.